

REPORT DOCUMENTATION PAGE

Form Approved
OMB No. 0704-0188

Public reporting burden for this collection of information is estimated to average 1 hour per response, including the time for reviewing instructions, searching existing data sources, gathering and maintaining the data needed, and completing and reviewing this collection of information. Send comments regarding this burden estimate or any other aspect of this collection of information, including suggestions for reducing this burden to Department of Defense, Washington Headquarters Services, Directorate for Information Operations and Reports (0704-0188), 1215 Jefferson Davis Highway, Suite 1204, Arlington, VA 22202-4302. Respondents should be aware that notwithstanding any other provision of law, no person shall be subject to any penalty for failing to comply with a collection of information if it does not display a currently valid OMB control number. **PLEASE DO NOT RETURN YOUR FORM TO THE ABOVE ADDRESS.**

1. REPORT DATE (DD-MM-YYYY) August 2012		2. REPORT TYPE Journal Article		3. DATES COVERED (From - To)	
4. TITLE AND SUBTITLE Functionalization of Fluoroalkyl Polyhedral Oligomeric Silsesquioxanes (F-POSS) (Post Print)				5a. CONTRACT NUMBER	
				5b. GRANT NUMBER	
				5c. PROGRAM ELEMENT NUMBER	
6. AUTHOR(S) Sean M. Ramirez, Yvonne J. Diaz, Raymond Campos, Timothy S. Haddad, Joseph M. Mabry				5d. PROJECT NUMBER	
				5e. TASK NUMBER	
				5f. WORK UNIT NUMBER Q0AD	
7. PERFORMING ORGANIZATION NAME(S) AND ADDRESS(ES) Air Force Research Laboratory (AFMC) AFRL/RQRP 10 E. Saturn Blvd Edwards AFB CA 93524-7680				8. PERFORMING ORGANIZATION REPORT NO.	
9. SPONSORING / MONITORING AGENCY NAME(S) AND ADDRESS(ES) Air Force Research Laboratory (AFMC) AFRL/RQRP 10 E. Saturn Blvd Edwards AFB CA 93524-7680				10. SPONSOR/MONITOR'S ACRONYM(S)	
				11. SPONSOR/MONITOR'S REPORT NUMBER(S) AFRL-RQ-ED-JA-2012-274	
12. DISTRIBUTION / AVAILABILITY STATEMENT Approved for public release; distribution unlimited					
13. SUPPLEMENTARY NOTES Journal article published in the American Chemical Society, ACS Symposium Series, Chapter 7, Aug 2012. PA Case Number: 12758; Clearance Date: 9/12/2012. © 2012 American Chemical Society The U.S. Government is joint author of the work and has the right to use, modify, reproduce, release, perform, display, or disclose the work.					
14. ABSTRACT Incompletely-condensed fluoroalkyl-functional Polyhedral Oligomeric SilSesquioxanes (F-POSS) have been synthesized via a scaleable three-step synthetic process with an overall yield of 52%. The primary byproduct of each step in the synthesis is the completely-condensed F-POSS starting material, which enables the recycling of the starting materials. The incompletely condensed structures were readily reacted with a variety of functional dichlorosilanes to introduce reactive or unreactive functionality and produce unsymmetrical F-POSS structures. Chemical structures were confirmed by elemental analysis, multinuclear NMR (1H, 13C, 19F, and 29Si), and FT-IR methods. Single crystal X-ray diffraction was used to elucidate the crystal structure of the precursor F-POSS disilanol. The functionalized F-POSS structures were found to possess variable solubility properties, generally superior to those of the closed-cage F-POSS starting material. Dynamic contact angle measurements of these compounds were examined using water and hexadecane as the wetting liquids. Copolymers of poly(methyl methacrylate) containing F-POSS were synthesized from methacrylate F-POSS macromers. These novel structures can be used as building blocks for the development of low surface energy materials.					
15. SUBJECT TERMS					
16. SECURITY CLASSIFICATION OF:			17. LIMITATION OF ABSTRACT	18. NUMBER OF PAGES	19a. NAME OF RESPONSIBLE PERSON Joseph Mabry
a. REPORT Unclassified	b. ABSTRACT Unclassified	c. THIS PAGE Unclassified			19b. TELEPHONE NO (include area code) 661 275-5857

Chapter 7

Functionalization of Fluoroalkyl Polyhedral Oligomeric Silsesquioxanes (F-POSS)

Sean M. Ramirez,^{*,1} Yvonne J. Diaz,¹ Raymond Campos,¹
Timothy S. Haddad,¹ and Joseph M. Mabry²

¹ERC Inc., Air Force Research Laboratory, Space & Missile Propulsion
Division, Edwards Air Force Base, California 93524-7680

²Air Force Research Laboratory, Space & Missile Propulsion Division,
Edwards Air Force Base, California 93524-7680

*E-mail: Sean.Ramirez.ctr@edwards.af.mil

Incompletely-condensed fluoroalkyl-functional Polyhedral Oligomeric Silsesquioxanes (F-POSS) have been synthesized *via* a scaleable three-step synthetic process with an overall yield of 52%. The primary byproduct of each step in the synthesis is the completely-condensed F-POSS starting material, which enables the recycling of the starting materials. The incompletely condensed structures were readily reacted with a variety of functional dichlorosilanes to introduce reactive or unreactive functionality and produce unsymmetrical F-POSS structures. Chemical structures were confirmed by elemental analysis, multinuclear NMR (¹H, ¹³C, ¹⁹F, and ²⁹Si), and FT-IR methods. Single crystal X-ray diffraction was used to elucidate the crystal structure of the precursor F-POSS disilanol. The functionalized F-POSS structures were found to possess variable solubility properties, generally superior to those of the closed-cage F-POSS starting material. Dynamic contact angle measurements of these compounds were examined using water and hexadecane as the wetting liquids. Copolymers of poly(methyl methacrylate) containing F-POSS were synthesized from methacrylate F-POSS macromers. These novel structures can be used as building blocks for the development of low surface energy materials.

Introduction

Designing materials with low surface energy and mechanical robustness has become a major objective in the scientific community. Various nano-fillers have been blended into polymers in order to improve overall system performance as non-wetting surfaces. Of these fillers, a sub-class of particles possessing long-chain fluoroalkyl groups, Fluoroalkyl Polyhedral Oligomeric Silsesquioxanes (F-POSS), has recently been developed and observed to be an excellent nano-filler for low surface energy applications (1–4). These compounds possess an inorganic silicon-oxygen core [SiO_{1.5}] with a periphery of long-chain fluorinated alkyl groups. These groups impact the surface morphology, crystallinity, and overall surface energy, which bestow F-POSS with several useful properties (3–6). A variety of chain lengths have been investigated to determine the optimal chain length for the lowest surface energy (Figure 1). Of these peripheral chain lengths, the fluorodecyl POSS compound possesses one of the lowest surface energy values known ($\gamma_{sv} = 9.3$ mN/m) for any crystalline solid (7). F-POSS compounds have been blended in polymer matrices and cast neat to produce superhydrophobic and superoleophobic surfaces (7–10). Dramatic improvements in water and oil repellency were observed when F-POSS was blended with perfluorocyclobutyl (PFCB) aryl ether polymers (11).

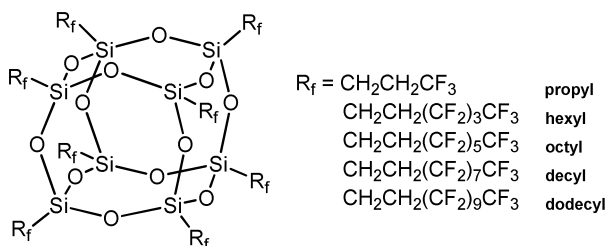


Figure 1. F-POSS peripheral chain lengths synthesized.

Neat films of F-POSS surfaces possess poor surface robustness and are susceptible to surface abrasion. To circumvent these issues, F-POSS have been physically blended with a variety of polymers (4, 5). However, the physical blending has illuminated certain issues in the incorporation of F-POSS in polymer matrices. For example, these composites are still prone to surface abrasion, mechanical robustness, and phase separation of the POSS domain. To date, there is no viable methodology to covalently attach F-POSS to a host polymer matrix, whereas non-fluorinated POSS structures have been chemically bound to polymer matrices (1, 11–15). An additional issue plaguing the long-chain fluoroalkyl POSS compounds is the limited range of solvents in which they are soluble. Previously, the selection has been limited to fluorinated solvents. To overcome these limitations, the development of a silanol functionalized incompletely-condensed (open-cage) F-POSS has been desired to enable new, robust, low surface energy hybrid materials. Incompletely-condensed silsesquioxane structures are used as models for silica (16), catalyst support (17), and precursors for silsesquioxane containing polymers (11). To date, a

viable synthetic strategy to produce long-chain F-POSS compounds possessing additional reactive or non-reactive functionality does not exist. There are few examples in the literature of short-chain incompletely condensed silsesquioxanes with functionality. For example, (3,3,3-trifluoropropyl)₇Si₇O₉(ONa)₃, has been derivatized with long-chain fluorinated trichlorosilanes to produce low surface energy materials (8). However, these shorter propyl chains do not possess the same magnitude of liquid repellency as longer fluoroalkyl chains (4). Also, the added functionality was a fluoroalkyl group and not an organic moiety with a reactive segment.

Herein, we report a simple approach to converted closed cage F-POSS into an incompletely condensed silsesquioxanes (18). This method follows the synthetic strategies developed by Feher and coworkers. Feher's work consisted of opening completely-condensed POSS cage edges through multistep syntheses to create silanols in varying degree *via* an acidic (19) or basic route (20). The acidic route was applied to F-POSS cages because it has proven successful for alkyl POSS cages.

Experimental

Materials

F-POSS (1) was synthesized according to literature procedure (4). Compounds 2-7 were synthesized according to previously described procedure (18). (3-Acryloxypropyl) methylchlorosilane (Gelest), vinylmethylchlorosilane (Gelest), hexafluorobenzene (C₆F₆, Synquest), 1,3-dichloro-1,2,2,3,3-pentafluoropropane (AK-225G, AGC Chemicals Americas), and hexadecane (Aldrich) were used without further purification, unless otherwise stated. All reactions were performed under a nitrogen atmosphere unless stated otherwise.

Characterization

Combustion analysis was performed by Atlantic Microlab, Inc. ¹H, ¹³C, ¹⁹F, and ²⁹Si NMR spectra were obtained on Bruker 300-MHz and 400-MHz spectrometers. An inverse gated 30° pulse with a 12 sec delay was used to acquire ²⁹Si NMR spectra. FT-IR spectra were taken on a Perkin Elmer Spectrum BX. Surface roughness was determined using a Digital Instruments Nanoscope IV (AFM) and a Veeco WykoNT930 optical profilometer. Size exclusion chromatography (SEC) was performed with a high-pressure liquid chromatography (HPLC, Agilent) system at a flow rate of 1.00 mL/min through two columns (Mixed pGel C and E) using THF as the carrier solvent. This was equipped with multi-angle light scatter (MALS, Dawn Helios Wyatt), viscometer (ViscoStar, Wyatt) and refractive index (RI, Optilab-rex, Wyatt) detectors. The RI detector was used to determine dn/dc values for the determination of absolute MW with the MALS detector. Surface measurements were followed according to literature procedure.

X-Ray Crystallography Data

Single crystals of compound **2** were grown from the slow evaporation of **2** in C₆F₆, resulting in clear platelets. Crystal data for **2** was collected at T=100.0 K using Kusing Bruker 3-circle, SMARTAPEX CCD with c-axis fixed at 54.748, running on SMART V 5.625 program (Bruker AXS: Madison, 2001). Graphite monochromated CuK α (λ = 1.54179 Å) radiation was employed for data collection and corrected for Lorentz and polarization effects using SAINT V 6.22 program (Bruker AXS: Madison, 2001), and reflection scaling (SADABS program, Bruker AXS: Madison, WI, 2001). Structure was solved by direct methods (SHELXL-97, Bruker AXS: Madison, 2000) and all non-hydrogen atoms refined anisotropically using full-matrix least-squares refinement on F². Hydrogen atoms were added at calculated positions. For **2**, M_r=, monoclinic, space group P2(1)/c, a=11.833(2) Å, b=57.141(11) Å, c=19.069(4) Å, α =90.00°, β =92.20(3)°, γ =90.00°, V= 12884(4) Å³, F(000)=7816, $\rho_{\text{calcd}}(Z=2)$ = 2.068 gcm⁻³, μ = 3.183 mm⁻¹, approximate crystal dimensions 0.60 x 0.35 x 0.20 mm³, θ range = 0.71 to 24.74°, 122186 measured data of which 21422 (R_{int} =0.0608, R_{σ} = 0.0379) unique with 3715 refined parameters, 14705 restraints were applied, final R indices [$I > 2\sigma(I)$]: R1=0.0915, $wR2$ =0.1918, R1=0.0857, $wR2$ =0.1893 (all data), GOF on F^2 =1.230. CCDC 843485 contains the supplementary crystallographic data for this paper. This data can be obtained free of charge from The Cambridge Crystallographic Data Centre via www.ccdc.cam.ac.uk/data_request/cif.

General Synthesis of F-POSS Monomers

A solution of **2** (4.00 g, 0.99 mmol), 3-acryloxypropylmethylchlorosilane (0.226 g, 0.99 mmol), and Et₃N (0.200 g, 1.95 mmol) were stirred together for 12 hr. During this time a white precipitate formed. The solution was then filtered and poured into ethyl acetate, at which time, a white solid precipitated (F-POSS). This solid was removed *via* filtration and the filtrate was concentrated, then dissolved in diethyl ether and filtered. The filtrate was collected and cooled to 0 °C affording a white precipitate. The precipitate was collected and dried under vacuum to afford a white powder (**7**) (1.9 g, 48%). ¹H NMR (300 MHz, (CD₃CD₂)₂O, ppm) δ 6.01 (s, 1H), 5.56 (s, 1H), 4.16 (t, 2H) 2.25 (m, 16H), 1.92 (s, 3H), 1.84 (m, 2H), 1.09 (m, 16H), 0.76 (t, 2H), 0.26 (s, 3H). ²⁹Si{¹H} NMR δ -18.1, -66.08, -68.64, -69.2 (1:2:4:2). ¹⁹F NMR -82.3 (3F), -116.9 (2F), -122.6 (6F), -123.7 (2F), -124.3 (2F), -127.3 (2F).

General Polymerization of F-POSS Monomers

Methyl methacrylate (MMA, 1.31 g, 13.1 mmol), **3** (0.36 g, 0.09 mmol), azobisisobutyronitrile (AIBN, 5 mg, 0.001 mmol) were dissolved in a C₆F₆:THF mixture (4:1). This solution was purged with nitrogen for 25 minutes to remove any oxygen and was immediately submerged in a 60°C oil bath for 18 hrs. The

resulting solution was precipitated in hexanes, filtered and dried to yield a fluffy white powder (0.93 g, 71%).

Results and Discussion

In order to successfully open the chemically resistant F-POSS, a three-step synthetic procedure was developed following a similar method first employed by Feher *et al* (18, 21, 22). The first step involved opening the F-POSS (**1**) cage with a trifluoromethane sulfonic acid (HOTf) to form the triflate intermediate compound **1a** (Figure 2). This reaction involves equilibrium between the open and closed-cage silsesquioxane frameworks, making the ^{29}Si NMR spectra complex. Compound **1a** can be observed with ^{29}Si resonances at -62.6, -65.0, and -66.7 ppm (Si ratio 2:2:4). Starting material is also observed with a strong peak at -66.3 ppm. To obtain the maximum amount of the desired ditriflate, this reaction was stopped at 75 minutes. If reaction time is extended, the HOTf will continue to attack the POSS cage framework, resulting in a complex mixture of triflate cages. This mixture of cages can be observed in ^{29}Si NMR (Figure 3). Attempts to isolate these additional cages have resulted in a reversion of this mixture to compound **1**. Unfortunately, the ditriflate is highly unstable and each attempt to isolate **1a** also resulted in a complete reversion to compound **1**. This has been attributed to the strong electron withdrawing effect of fluorodecyl chains and difficulty in finding a suitable solvent for compound **1a** besides C_6F_6 .

As a result of the instability of the ditriflate compound, $\text{NBut}_4\text{HSO}_4$ was immediately added to the reaction mixture to bridge any disilanol functionality with a sulfate group (Figure 4). This results in the reaction mixture separating into two liquid layers; a yellow aqueous layer and a clear, colorless fluorinated solvent layer containing both **1b** and **1**. The bridging sulfate moiety appears to stabilize the electron-withdrawing F-POSS cage framework, leading to another NMR observed intermediate with ^{29}Si resonances at -64.5, -65.7, and -67.3 ppm (Si ratio 2:2:4) (Figure 5). A viable isolation procedure for intermediate **1b** has not been attained and isolation attempts have resulted in complete reversion to compound **1**. Similar to the previous reaction, the higher density clear fluorinated solvent layer from the reaction mixture is used “as is” for the next reaction step.

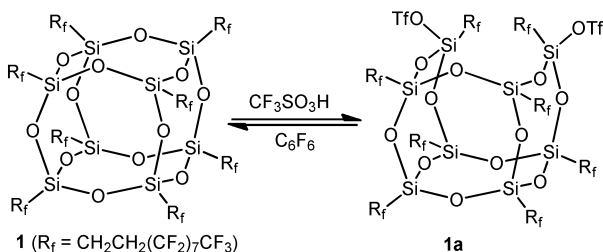


Figure 2. Cage opening reaction with HOTf.

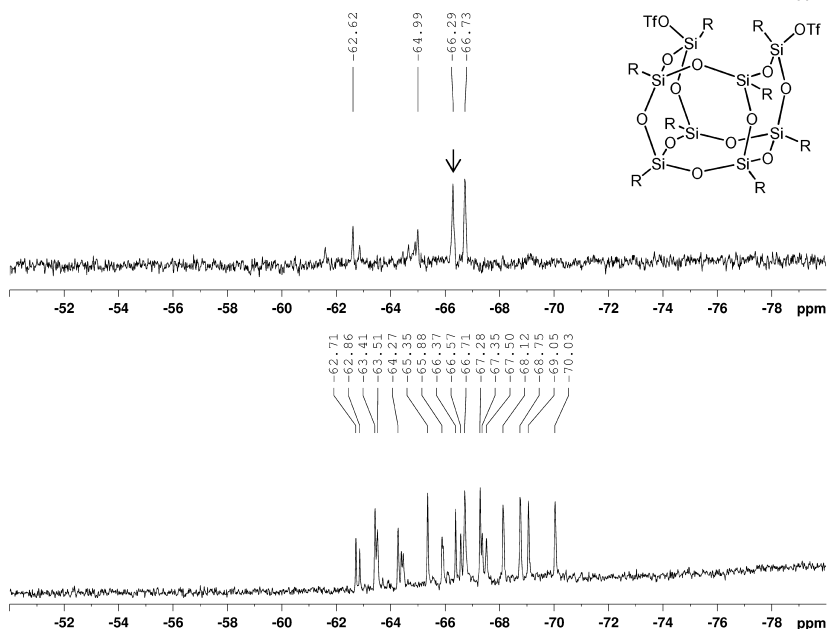


Figure 3. ^{29}Si NMR of **1a** and **1** in C_6F_6 (top). Open cage mixture of unidentified POSS structures and open cages if reaction proceeds for extended periods of time (bottom). Arrow points to unreacted compound **1**.

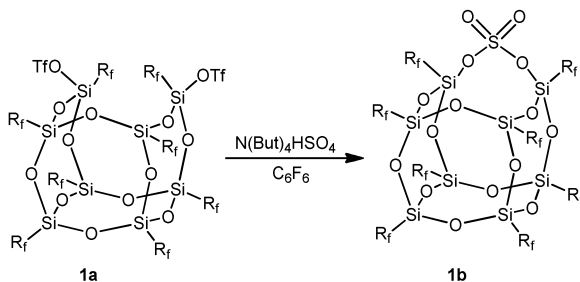


Figure 4. Bridged sulfate reaction of reaction intermediates **1a** and **1b**.

The bridged sulfate reaction mixture is subsequently added to a polar fluorinated solvent/water mixture to convert **1b** to disilanol F-POSS (**2**) in good overall yield (*ca.* 53%) (Figure 6). The use of a polar fluorinated solvent is vital for this reaction to proceed. This solvent allows for the introduction of water in a highly fluorinated environment. The disilanol compound **2** is purified away from any residual compound **1** through the solubility differences between the open and closed structures in C_6F_6 and ethyl acetate mixtures. Compound **1** precipitates from this solution mixture and the soluble compound **2** is precipitated from a CHCl_3 solution. This step also helps remove any residual resinous products that

might have formed during the reaction. The main side product produced during each step was compound **1** and this was subsequently recycled. Combustion analysis and multinuclear NMR (^1H , ^{13}C , ^{19}F , and ^{29}Si) were used to confirm the structure of **2**. The ^{29}Si NMR spectrum of **2** displayed peaks at -58.8, -65.6, -68.0 ppm, with an integration ratio of 2:2:4, due to the C_{2v} symmetry of the silsesquioxane (Figure 7). The peak at -59 ppm was attributed to the silanol group on the POSS structure.

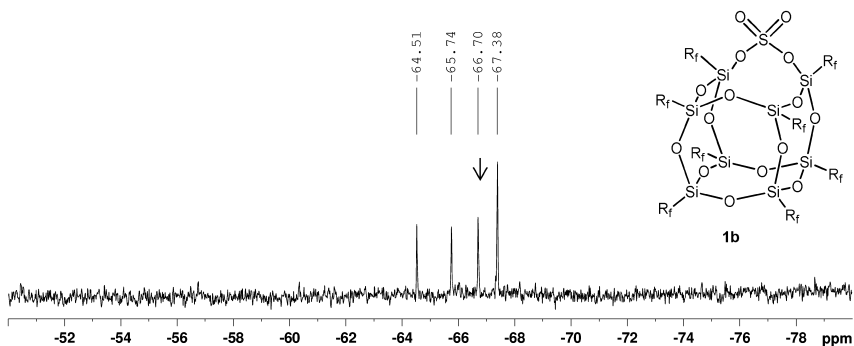


Figure 5. ^{29}Si NMR of **1b** and **1**. Arrow points to unreacted compound **1** in C_6F_6 .

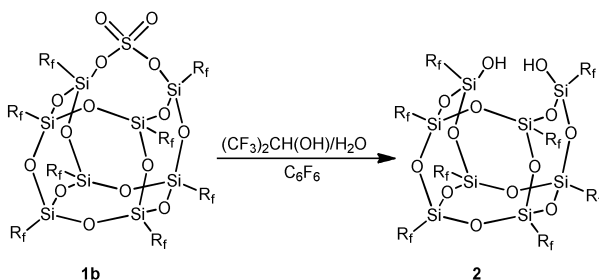


Figure 6. Final reaction of bridged sulfate to disilanol.

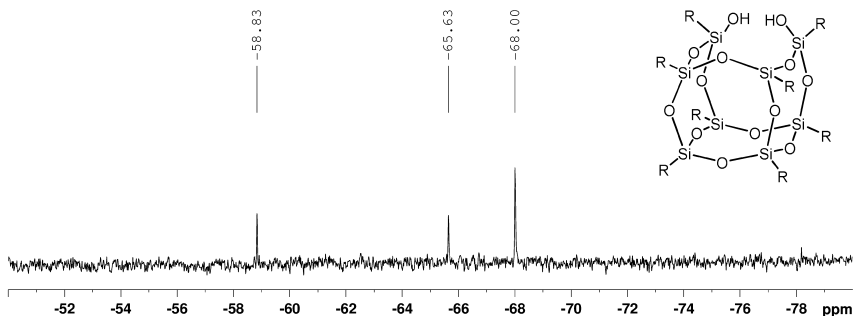


Figure 7. ^{29}Si NMR of compound **2** in C_6F_6 .

Single crystal X-ray diffraction was used to confirm the structure and absolute stereochemistry of compound **2** (Figure 8). The crystal structure for compound **2** was obtained from crystals grown by the slow evaporation of a C₆F₆ solution. This yielded long clear, colorless, plate-like crystals. The structure was determined to be Monoclinic P2(1)/c with a lattice volume of 12884 Å³. The structure contains rigid, helical-like fluoroalkyl chains, similar to compound **1**, which are attached to the open Si-O frame-work via methylene groups. The structure confirms the Si integration values established by ²⁹Si NMR spectra with a Si ratio of 2:2:4. This crystal structure contains substantial disorder along the fluorinated chains, due to the mobility of the fluoroalkyl groups.

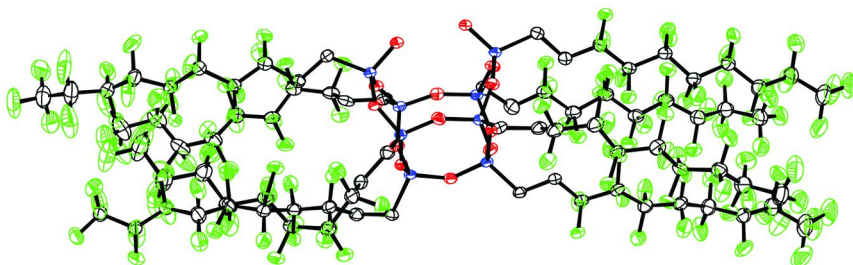


Figure 8. ORTEP representation of compound **2** at 100 K. The fluorinated chains contain substantial disorder. Thermal ellipsoids at 50%. Green F, Black C, Red O, Blue Si. (Hydrogen atoms and disordered segments are omitted for clarity).

The crystal packing of compound **2** reveals a dimeric structure with two F-POSS cages forming intermolecular hydrogen bonds between silanol groups on adjacent cages (Figure 9). A dimeric contact is established from the intermolecular silanols at a distance of 2.798 Å. These intermolecular silanols are slightly closer than intramolecular silanols at a distance of 2.810 Å. Interestingly, this observed hydrogen bonding forms an eight-membered ring from the O-H...O interaction. Additional groups have observed intermolecular hydrogen bonding between silanols on incompletely-condensed silsesquioxanes for POSS silanols (12). This interaction is believed to help stabilize this disilanol structure in solution as well. The disilanol F-POSS structure has a limited stability in solvents other than C₆F₆. For example, hydrochlorofluorocarbon solvent, Asahiklin-225®, is an excellent solvent for closed cage F-POSS compounds, but compound **2** will rapidly revert to compound **1** when dissolved. The reversion of compound **2** to **1** is attributed to a dehydration of adjacent silanols (Figure 10). Compound **2** is stable in hexafluorobenzene possibly due to the dimerization of the cage in solution.

The endo, endo disilanol on the open POSS framework were found to be reactive to several dichlorosilanes (Figure 11). A variety of functional dichlorosilanes were added to compound **2** to produce a small library of compounds **3-7** (Figure 12). For example, the condensation of **2** with (3-acryloxypropyl) methylchlorosilane in the presence of triethylamine

produced compound **6** (ca. 67% yield) with the loss of HCl. The primary side product isolated during the reaction was the initial starting material, compound **1**. Multinuclear NMR (^1H , ^{13}C , ^{19}F , and ^{29}Si), FT-IR, and combustion analysis were used to confirm the structure of **6**. The ^{29}Si resonances were -17.8, -65.7, -68.2, and -68.9 ppm, with a ratio of 1:2:4:2 (Figure 12). The resonance at -17.8 ppm is attributed the new Si atom in the POSS framework. A new Si resonance was observed in all the ^{29}Si NMRs of the synthesized F-POSS structures. Interestingly, the functionalization of the POSS cage influences the immediate Si-CH₂ group as observed in ^{13}C NMR (Figure 13). A ratio of 2:4:2 from the symmetry of the POSS cage framework (Figure 14). Strong C-H stretches observed around 2950 and 2860 cm^{-1} in the FT-IR spectrum also confirmed the presence of the added hydrocarbon chains.

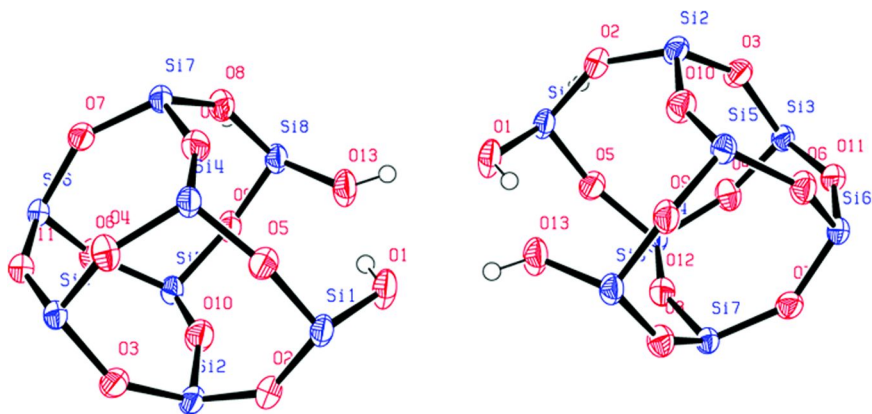


Figure 9. ORTEP representation of compound **2** in crystal form at 100 K showing the close proximity of disilanol. Thermal ellipsoids at 50%. Green F, Black C, Red O, Blue Si. (Hydrogen atoms and fluorinated chains are omitted for clarity).

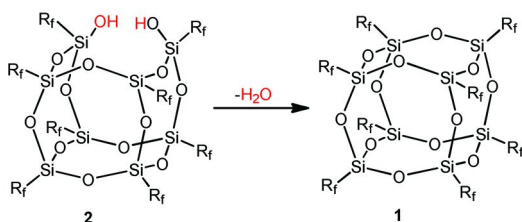


Figure 10. Representation of reversion of compound **2** to **1** via dehydration.

Once functionalized, the stability of the F-POSS cage improves substantially. These structures no longer revert to their parent compound **1** and their solubility properties change dramatically dependent on functional moiety. For example, the long hydrocarbon chains present in compound **3** expanded F-POSS solubility

to include non-fluorinated solvents, such as Et₂O and CHCl₃. Additional modifications, such as the acrylate and methacrylate moieties on structures **6** and **7**, were sufficient enough to expand the solubility of F-POSS to non-fluorinated solvents, such as Et₂O. However, phenyl (**4**) and vinyl (**5**) groups did not improve the solubility of F-POSS in non-fluorinated solvents. This was attributed to rigidity and size of the groups. Solubility increases were improved overall with the addition of an aliphatic chain to the F-POSS structure. Neither asymmetric nor symmetric functionality seem to have a preferential influence on the solubility of these structures (Figure 15).

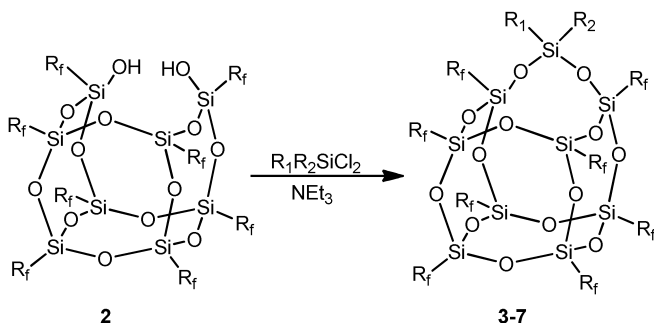


Figure 11. Reaction of disilanol F-POSS with dichlorosilanes to produce functional F-POSS compounds.

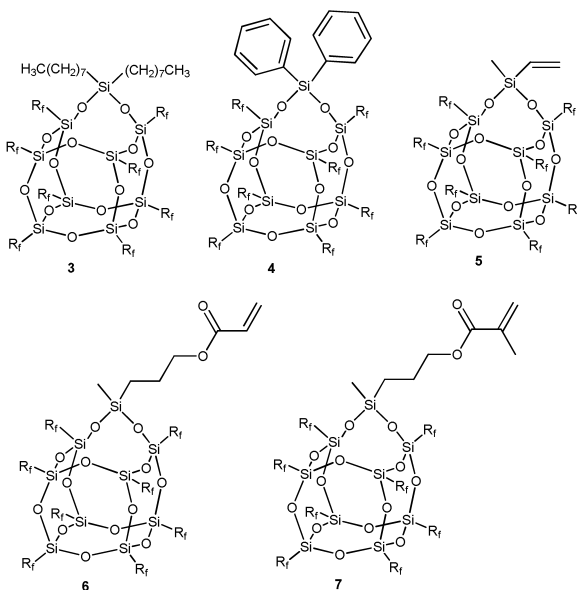


Figure 12. Compounds synthesized from reaction disilanol F-POSS and dichlorosilanes.

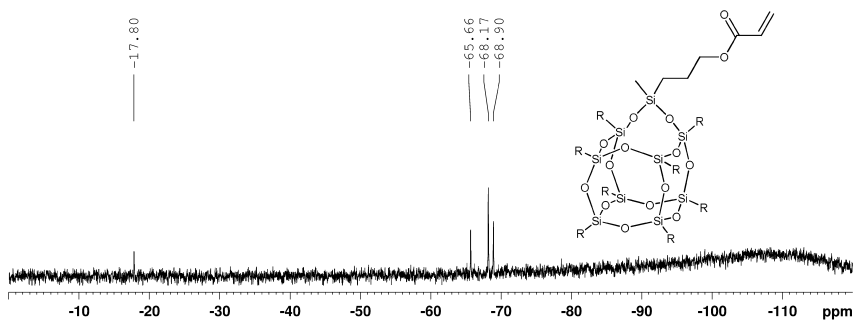


Figure 13. ^{29}Si NMR of compound **6** in C_6F_6 .

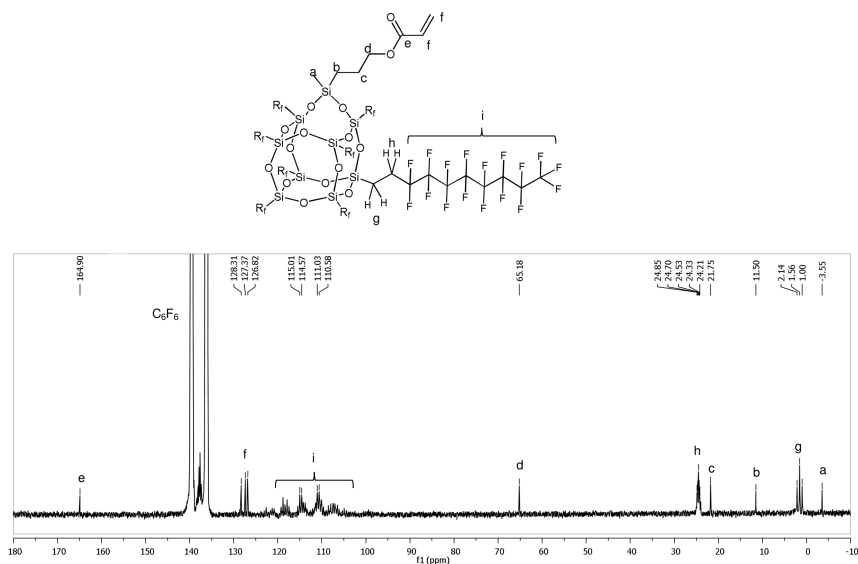


Figure 14. ^{13}C NMR of compound **6** in C_6F_6 . Peak at 128.3 ppm is residual C_6H_6 present in C_6F_6 .

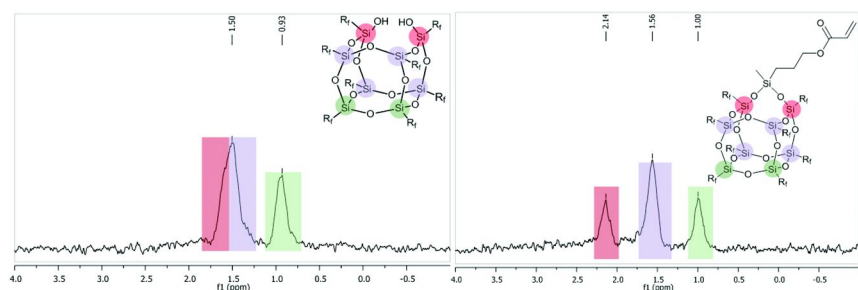


Figure 15. Zoom in of ^{13}C NMR of compound **1** (left) and compound **6** (right) in C_6F_6 . Highlights show the symmetry of the Si cage framework and how functionalization can influence the chemical shifts for Si- $\underline{\text{C}}\text{H}_2$.

The desirable low surface energy characteristics of F-POSS are partially due to the long chain fluoroalkyl peripheral on the POSS cage framework. To study the influence of functionality on the F-POSS, both static and dynamic contact angle measurements of water and hexadecane were taken of neat films spun cast on SiO₂ wafers (Table 1) (18). Water was used to determine the hydrophobicity and hexadecane for oleophobicity. Samples were cast as smooth films to minimize any influence of surface roughness and topology. Surface roughness was measured (< 5 nm rms) with atomic force microscopy and optical profilometry. Dynamic contact angle measurements were used to help determine the effect of functionality on F-POSS. There were no observable adverse effects from the open cage F-POSS framework of compound **2** on non-wetting behavior. This was attributed to the dimeric structure of **2** and the shielding of the silanols from water and hexadecane. A slight increase in contact angle hysteresis, $\theta_{\text{rec}} - \theta_{\text{adv}}$, for the modified compounds (**3**, **5-7**) was observed when wetted with water. This slight increase was not observed for compounds wetted with hexadecane except for compound **3**. Compound **3** contains two long aliphatic (octyl) chains that potentially favor interaction with a long-chain organic solvent, such as hexadecane. Compounds **2** and **4** displayed the lowest hexadecane contact angle hysteresis values of all compounds and compound **4** possessed a sliding angles of $\sim 7^\circ$ with hexadecane (Figure 16e). These initial measurements provide the platform for further study of these systems with additional solvents.

Table 1. Dynamic contact angle measurements

<i>Compound</i>	<i>Water</i>		<i>Hexadecane</i>	
	(θ_{adv})	(θ_{rec})	(θ_{adv})	(θ_{rec})
F-POSS	124 ± 0.5°	109.6 ± 0.7°	79.1 ± 0.4°	65.1 ± 0.5°
2	116.8 ± 0.4°	111 ± 0.6°	77.4 ± 0.4°	74.4 ± 0.8°
3	117.9 ± 0.5°	95.5 ± 0.4°	69.1 ± 1.2°	23.1 ± 1.2°
4	116.2 ± 0.4°	110.5 ± 0.5°	76.0 ± 0.8°	73.2 ± 0.4°
5	116.2 ± 0.4°	100.6 ± 0.8°	78.4 ± 0.3°	70.6 ± 2.3°
6	118.2 ± 1.0°	90.6 ± 1.0°	76.8 ± 0.3°	64.8 ± 1.0°
7	117.1 ± 0.6°	93.8 ± 1.5°	78.1 ± 0.4°	63.0 ± 1.2°

After determining the influence of functionality on the F-POSS surface properties, the next step was to investigate the reactivity of the functional group on the F-POSS framework. The methacrylate based F-POSS compound **7** was examined using copolymerization with methyl methacrylate (MMA) *via* free radical polymerization. Unfortunately, any attempts at homopolymerization resulted in the starting macromer with no sign of polymerization. This was attributed to the steric hindrance of the MMA moiety on the F-POSS frame to polymerize with another bulky macromer. To circumvent this problem, copolymerizations with MMA were explored at varying weight ratio percentages of F-POSS to MMA (Figure 17). These initial polymerizations were performed at a low molar ratio of 7:MMA (1:144) due to the large molecular weight of compound **7** (4,178 g/mol). Multinuclear NMR and size exclusion chromatography (SEC)

was used to characterize (^1H , ^{19}F) the polymer. ^1H NMR revealed resonance signals at 0.5 – 2 ppm and 3.6 ppm which were attributed to PMMA. The resonances observed in the ^{19}F NMR spectra (-81.1, -109.9, -116.5, -122.3, -123.1, -124.2, -126.9 ppm) were attributed to the fluorinated chains on F-POSS (Figure 1). Molecular weight of the polymers obtained range from 35,000 to 45,000 g/mol with polydispersity indices ~ 1.4 . These polymers were found to be soluble in organic solvents such as tetrahydrofuran and chloroform. Currently a more in-depth analysis of these polymerizations is being undertaken.

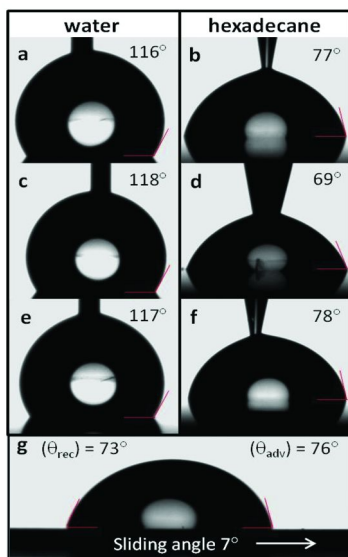


Figure 16. Static contact angles of smooth surfaces of compounds 2 (a) and (b), 3 (c) and (d), and 4 (e) and (f). Image of hexadecane droplet (10 μL) rolling off surface coated with compound 4 (e).

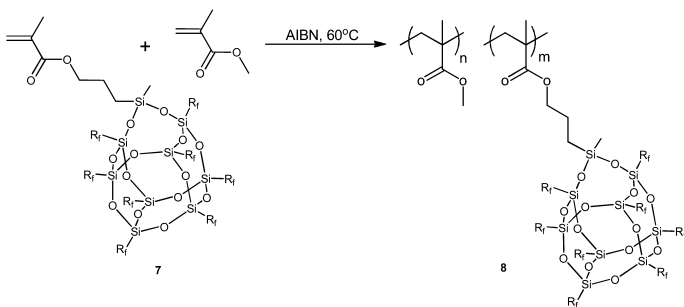


Figure 17. Free radical copolymerization of compound 7 with MMA.

Conclusion

Disilanol F-POSS was synthesized from the fully condensed F-POSS in a three-step reaction process. The disilanol F-POSS crystal structure indicates the silanol groups are hydrogen bonded *via* intra- and intermolecular interactions. The disilanol structure was demonstrated to be reactive toward dichlorosilanes, enabling the production of a variety of functional F-POSS structures, which were found to display similar wetting properties to unmodified F-POSS. Copolymers of MMA and methacrylate F-POSS were prepared, demonstrating that functional groups tethered to F-POSS are still reactive. Thus, a novel tunable structure now provides unprecedented access to fluorinated building blocks for low surface energy materials. The methacrylate and acrylate monomers are currently being investigated in a variety of copolymers and are expected to deliver new robust, abrasion resistant, superhydrophobic, and oleophobic material properties.

Acknowledgments

We gratefully acknowledge the Air Force Office of Scientific Research and the Air Force Research Laboratory, Propulsion Directorate for financial support. We thank Peter Müller at the Massachusetts Institute of Technology (MIT) and the American Crystallography Association (ACA) summer course for their assistance with small molecule X-ray crystal structure determination and refinement.

References

1. Cordes, D. B.; Lickiss, P. D.; Rataboul, F. *Chem. Rev.* **2010**, *110* (4), 2081–2173.
2. Lickiss, P. D.; Rataboul, F. *Adv. Organomet. Chem.* **2008**, *57*, 1.
3. Mabry, J. M.; Vij, A.; Iacono, S. T.; Viers, b. D. *Angew. Chem., Int. Ed.* **2008**, *47*, 4137–4140.
4. Iacono, S. T.; Budy, S. M.; Mabry, J. M.; Smith, D. W., Jr. *Macromolecules* **2007**, *40*, 9517–9522.
5. Tuteja, A.; Choi, W.; Mabry, J. M.; McKinley, G. H.; Cohen, R. E. *Proc. Natl. Acad. Sci. U.S.A.* **2008**, *105*, 18200–18205S18200/1-S18200-29.
6. Tuteja, A.; Choi, W.; Ma, M.; Mabry, J. M.; Mazzella, S. A.; Rutledge, G. C.; McKinley, G. H.; Cohen, R. E. *Science* **2007**, *318*, 1618–1622.
7. Chhatre, S. S.; Guardado, J. O.; Moore, B. M.; Haddad, T. S.; Mabry, J. M.; McKinley, G. H.; Cohen, R. E. *ACS Appl. Mater. Interfaces* **2010**, *2*, 3544–3554.
8. Iacono, S. T.; Vij, A.; Grabow, W.; Smith, D. W., Jr.; Mabry, J. M. *Chem. Commun.* **2007**, 4992–4994.
9. Choi, W.; Tuteja, A.; Chhatre, S.; Mabry, J. M.; Cohen, R. E.; McKinley, G. H. *Adv. Mater.* **2009**, *21*, 2190–2195.
10. Iacono, S. T.; Budy, S. M.; Smith, D. W., Jr.; Mabry, J. M. *J. Mater. Chem.* **2010**, *20*, 2979–2984.
11. Haddad, T. S.; Lichtenhan, J. D. *Macromolecules* **1996**, *29* (22), 7302–7304.

12. Haddad, T. S.; Viers, B. D.; Phillips, S. H. *J. Inorg. Organomet. Polym. Mater.* **2001**, *11* (3), 155–164.
13. Pielichowski, K. N.; Njuguna, J.; Janowski, B.; Pielichowski, J. *Adv. Polym. Sci.* **2006**, *201*, 225–296.
14. Phillips, S. H.; Haddad, T. S.; Tomczak, S. J. *Curr. Opin. Solid State Mater. Sci.* **2004**, *8*, 21–29.
15. Koh, K.; Sugiyama, S.; Morinaga, T.; Ohno, K.; Tsujii, Y.; Fukuda, T.; Yamahiro, M.; Iijima, T.; Oikawa, H.; Watanabe, K.; Miyashita, T. *Macromolecules* **2005**, *38*, 1264–1270.
16. Feher, F. J.; Newman, D. A.; Walzer, J. F. *J. Am. Chem. Soc.* **1989**, *111* (5), 1741–1748.
17. Feher, F. J.; Tajima, T. L. *J. Am. Chem. Soc.* **1994**, *116* (5), 2145–2146.
18. Ramirez, S. M.; Diaz, Y. J.; Campos, R.; Stone, R. L.; Haddad, T. S.; Mabry, J. M. *J. Am. Chem. Soc.* **2011**, *133* (50), 20084–20087.
19. Feher, F. J.; Nguyen, F.; Soulivong, D.; Ziller, J. W. *Chem. Commun.* **1999**, 1705–1706.
20. Feher, F. J.; Terroba, R.; Ziller, J. W. *Chem. Commun.* **1999**, 2309–2310.
21. Feher, F. J.; Soulivong, D.; Nguyen, F.; Ziller, J. W. *Angew. Chem., Int. Ed.* **1998**, *37* (19), 2663–2667.
22. Feher, F. J.; Soulivong, D.; Nguyen, F. *Chem. Commun.* **1998**, 1279–1280.
23. Liu, H.; Kondo, S.; Tanaka, R.; Oku, H.; Unno, M. *J. Organomet. Chem.* **2008**, *693*, 1301–1308.